

# 1 Surface Equilibration Mechanism Controls the Stability of a Model 2 Codeposited Glass Mixture of Organic Semiconductors

3 Shinian Cheng, Yejung Lee, Jinguang Yu, Lian Yu, and M. D. Ediger\*



Cite This: <https://doi.org/10.1021/acs.jpcllett.3c00728>



Read Online

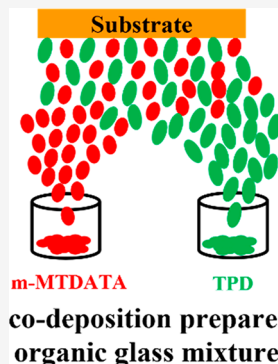
ACCESS |

Metrics & More

Article Recommendations

Supporting Information

4 **ABSTRACT:** While previous work has identified the conditions for preparing ultrastable single-  
5 component organic glasses by physical vapor deposition (PVD), little is known about the stability of  
6 codeposited mixtures. Here, we prepared binary PVD glasses of organic semiconductors, TPD (*N,N'*-  
7 Bis(3-methylphenyl)-*N,N'*-diphenylbenzidine) and m-MTDATA (4,4',4''-Tris[phenyl(m-tolyl)-  
8 amino]triphenylamine), with a 50:50 mass concentration over a wide range of substrate temperatures  
9 ( $T_{\text{sub}}$ ). The enthalpy and kinetic stability are evaluated with differential scanning calorimetry and  
10 spectroscopic ellipsometry. Binary organic semiconductor glasses with exceptional thermodynamic and  
11 kinetic stability comparable to the most stable single-component organic glasses are obtained when  
12 deposited at  $T_{\text{sub}} = 0.78\text{--}0.90T_g$  (where  $T_g$  is the conventional glass transition temperature). When  
13 deposited at  $0.94T_g$ , the enthalpy of the m-MTDATA/TPD glass equals that expected for the  
14 equilibrium liquid at that temperature. Thus, the surface equilibration mechanism previously advanced  
15 for single-component PVD glasses is also applicable for these codeposited glasses. These results  
16 provide an avenue for designing high-performance organic electronic devices.



17 **G**lasses play a central role in modern technologies,  
18 including communications,<sup>1</sup> pharmaceuticals,<sup>2</sup> and or-  
19 ganic electronics.<sup>3</sup> They are amorphous solids with macro-  
20 scopic homogeneity and nearly unlimited compositional  
21 flexibility. These features make glasses preferable to crystalline  
22 materials in some applications, such as organic light emitting  
23 diode (OLED) displays. The active layers in OLEDs are  
24 organic semiconductor glasses. The macroscopic homogeneity  
25 of glasses ensures smooth surfaces and uniform performance in  
26 all pixels, while the compositional flexibility of the glassy matrix  
27 facilitates the preparation of well-mixed emissive layers with  
28 tunable composition. A fundamental challenge for glass  
29 materials is their long-time stability.<sup>4,5</sup> Due to their non-  
30 equilibrium nature, glasses can either physically age<sup>6</sup> over time  
31 or undergo crystallization if chemical degradation is  
32 prevented.<sup>7</sup> Both may lead to degradation of the performance  
33 of the OLED device and reduce lifetime.<sup>8</sup> Therefore, it is  
34 practically important to produce glass materials with highly  
35 enhanced stability.

36 Recent studies have demonstrated that physical vapor  
37 deposition is an excellent technique to prepare glasses with  
38 exceptional thermodynamic and kinetic stability.<sup>9-12</sup> In  
39 addition, such ultrastable PVD glasses also exhibit high  
40 density,<sup>13</sup> enhanced photostability<sup>14,15</sup> high resistance to  
41 crystallization,<sup>16</sup> and high mechanical moduli.<sup>17,18</sup> These  
42 desirable properties cannot be obtained using other prepara-  
43 tion techniques. It is hypothesized that surface mobility is  
44 responsible for the formation of these ultrastable glasses  
45 prepared from PVD.<sup>11</sup> The strongly enhanced mobility at the  
46 glass surface allows molecules to find low energy configurations  
47 before being buried by further deposition.<sup>11</sup> This surface

equilibrium mechanism has been supported by theoretical<sup>48</sup>  
work,<sup>19,20</sup> computer simulations,<sup>21-23</sup> and direct surface<sup>49</sup>  
mobility measurements.<sup>24-27</sup> With a few exceptions,<sup>28-30</sup>  
however, the study of the stability of PVD organic glasses<sup>51</sup>  
has been limited to single-component systems.<sup>52</sup>

Some fundamental issues remain to be addressed regarding<sup>53</sup>  
the stability of the PVD glass mixtures. It is not clear whether a<sup>54</sup>  
mixture should form an ultrastable glass, even when the two<sup>55</sup>  
components individually form ultrastable glasses. Based on the<sup>56</sup>  
knowledge from single-component PVD glasses, high mobility<sup>57</sup>  
at the surface is the key for molecules to find low energy<sup>58</sup>  
configurations and form ultrastable glasses. However, it may be<sup>59</sup>  
impossible to find a proper deposition temperature, at which<sup>60</sup>  
both components for codeposition have high surface mobility<sup>61</sup>  
simultaneously, especially when they have a large difference in<sup>62</sup>  
 $T_g$  values. In addition, even if the two pure components can<sup>63</sup>  
have high enough surface mobility at a given temperature,<sup>64</sup>  
immiscibility or the capability to form hydrogen bonds<sup>65</sup>  
between components (which would lower surface mobility)<sup>66</sup>  
may block the formation of ultrastable mixtures. Very recent<sup>67</sup>  
work reported that codeposited organic semiconductor glasses<sup>68</sup>  
of 8-hydroxyquinolinolato-lithium (Liq) and 4,7-diphenyl-<sup>69</sup>

Received: March 17, 2023

Accepted: April 26, 2023

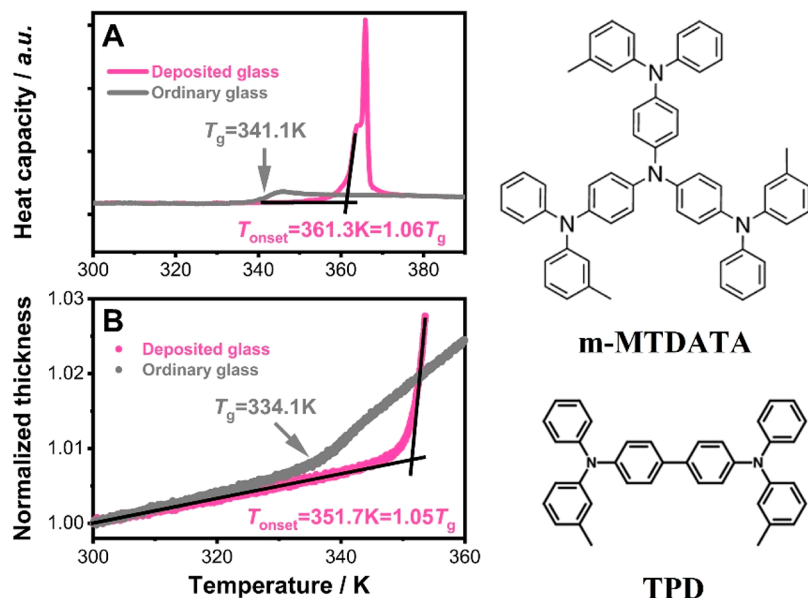


**Figure 1.** Temperature scanning experiments to determine the kinetic stability of codeposited m-MTDATA/TPD glasses with a mass ratio of 50:50. The binary glasses were prepared at  $T_{\text{sub}} = 300\text{ K}$  with a deposition rate  $0.42 \pm 0.03\text{ nm/s}$ . A) Heat capacity as a function of temperature determined from DSC measurements in the heating process with  $10\text{ K/min}$ ; B) Normalized film thickness as a function of temperature determined from ellipsometry ramping measurements at a heating rate of  $1\text{ K/min}$ . The film thickness is normalized at  $300\text{ K}$ .

70 1,10-phenanthroline (BPhen) do not show ultrastable properties (e.g., higher density).<sup>30</sup>

71 Understanding the properties of PVD glass mixtures is  
72 important for the technology. PVD is the standard route to  
73 prepare glassy layers of organic semiconductors in OLEDs and  
74 these layers are often mixtures. For example, the light-emitter  
75 layer is generally a glassy mixture of light-emitting molecules  
76 dispersed in a host.<sup>31–33</sup> Recent studies have indicated that  
77 OLEDs prepared with ultrastable vapor-deposited glass layers  
78 show extended device lifetime.<sup>34,35</sup> Thus, it is an important  
79 goal to understand the physical mechanisms controlling the  
80 stability of vapor-deposited glass mixtures and to identify the  
81 deposition conditions that produce highly stable multi-  
82 component glasses.

83 To enrich our understanding of multicomponent PVD  
84 glasses, we codeposited binary glasses of organic semi-  
85 conductors: m-MTDATA and TPD, in a wide substrate  
86 temperature ( $T_{\text{sub}}$ ) range. The two components selected can  
87 form ultrastable glasses as neat materials.<sup>36</sup> Differential  
88 scanning calorimetry and spectroscopic ellipsometry were  
89 applied to evaluate the enthalpies and kinetic stabilities of the  
90 PVD mixtures. In this work, we focused our attention on  
91 nondilute mixtures with a mass ratio near 50:50, as we  
92 anticipate that this is the regime in which ultrastable glass  
93 formation is most challenging. We found that the stability of  
94 codeposited m-MTDATA/TPD glasses is controlled by  $T_{\text{sub}}/T_g$   
95 (where  $T_g$  is the conventional glass transition temperature)  
96 in the same manner as single-component PVD organic glasses.  
97 When codeposited at  $T_{\text{sub}} = 0.78\text{--}0.90T_g$ , the most stable  
98 binary glasses are formed with an onset temperature being 5%  
99 higher than the conventional glass transition temperature,  
100 which is comparable to the most stable single-component  
101 organic glasses. Interestingly, the enthalpy of m-MTDATA/  
102 TPD glass deposited at  $0.94T_g$  is equal to that expected for the  
103 equilibrium liquid at that temperature. All these results are  
104 consistent with the surface equilibration mechanism previously  
105 advanced to understand single-component PVD glasses.

The DSC results in Figure 1A demonstrate that the codeposited m-MTDATA and TPD (chemical structures shown in Figure 1) glass mixture with a 50:50 mass ratio prepared at  $T_{\text{sub}} = 300\text{ K}$  is kinetically much more stable than the corresponding liquid-cooled glass. The results for the as-deposited sample obtained in the initial heating process are presented in pink. After the as-deposited glass is completely transformed into the liquid state, the same sample is cooled by  $10\text{ K/min}$  to form the corresponding liquid-cooled glass and then heated again, yielding the gray data. As shown in Figure 1A, the devitrification process for both deposited and liquid-cooled glass is accompanied by a significant increase in heat capacity. The onset temperature ( $T_{\text{onset}}$ ) where the as-deposited glass starts to transform is  $361.3\text{K}$ , while the glass transition temperature ( $T_g$ ) characterized using the midpoint convention for the corresponding liquid-cooled glass is  $341.1\text{K}$ . This  $20.2\text{ K}$  difference suggests that a much higher temperature is required for the vapor-deposited sample to disrupt its glassy molecular packing, a straightforward indication of higher kinetic stability for the codeposited m-MTDATA/TPD glass. It should be emphasized that the as-deposited films are fully amorphous. The absence of crystalline material is confirmed by grazing-incidence wide-angle X-ray scattering (GIWAXS) and DSC measurements (Figures S1 and S2).

One challenge in performing calorimetric measurements on thin vapor-deposited glasses is to introduce sufficient sample mass for good thermal signals. Rodríguez-Tinoco et al. addressed this issue by using aluminum foil as the substrate and then folding the foil with deposited glass into a DSC pan. In this work, we used gold foil rather than aluminum because of its better thermal conductance. We codeposited a  $1200\text{ nm}$  organic film onto a  $1.8 \times 1.8\text{ cm}^2$  gold foil; the foil mass was about  $0.4\text{ mg}$ , while the sample mass was about  $0.5\text{ mg}$ . As shown in Figure 1A, this mass is sufficient to obtain good glass transition thermal signals for our samples.

143 Ellipsometry measurements reveal consistent results with the  
 144 calorimetric experiments. Figure 1B shows the normalized film  
 145 thickness as a function of temperature for a codeposited m-  
 146 MTDATA/TPD (50:50) glass mixture at  $T_{\text{sub}} = 300$  K. The  
 147 film thickness for both as-deposited and liquid-cooled glasses  
 148 increases linearly with temperature due to thermal expansion.  
 149 A sharp deviation from this linear dependence was observed  
 150 when the samples started to expand as they transform into a  
 151 supercooled liquid. In the ellipsometry data, the obtained  $T_{\text{onset}}$   
 152 for codeposited m-MTDATA/TPD glass is 17.6 K higher than  
 153 the  $T_g$  for the liquid-cooled glass, consistent with high kinetic  
 154 stability. It is expected that the absolute transition temper-  
 155 atures measured by ellipsometry are somewhat lower than  
 156 those measured by calorimetry due to the lower heating rate  
 157 employed.

158 The ratio  $T_{\text{onset}}/T_g$  is often used to quantify the kinetic  
 159 stability of vapor-deposited glasses.<sup>38</sup> For the codeposited m-  
 160 MTDATA/TPD glasses, calorimetry and ellipsometry mea-  
 161 surements show good agreement, with  $T_{\text{onset}}/T_g$  equal to 1.06  
 162 from calorimetric experiments and 1.05 from ellipsometry  
 163 measurements. Interestingly,  $T_{\text{onset}}/T_g = 1.05\text{--}1.06$  is con-  
 164 sistent with the values found in the most stable single-  
 165 component PVD organic glasses.<sup>38</sup> Furthermore, the  $T_{\text{sub}} =$   
 166 300 K used to create the ultrastable m-MTDATA/TPD glasses  
 167 is equal to  $0.88T_g$  located in the optimal temperature region  
 168 (i.e.,  $0.78\text{--}0.90T_g$ ) for preparing single-component ultrastable  
 169 organic glasses.<sup>38</sup>

170 The results above suggest that the surface equilibration  
 171 mechanism previously advanced for single-component glasses  
 172 may be applied to understand the kinetic stability of  
 173 codeposited m-MTDATA/TPD glasses. To test this hypoth-  
 174 esis, we codeposited m-MTDATA/TPD mixtures with the  
 175 same mass ratio of 50:50 at five additional substrate  
 176 temperatures ranging from 210 to 340 K. We present the  
 177 DSC results for these codeposited glasses in Figure 2A and the

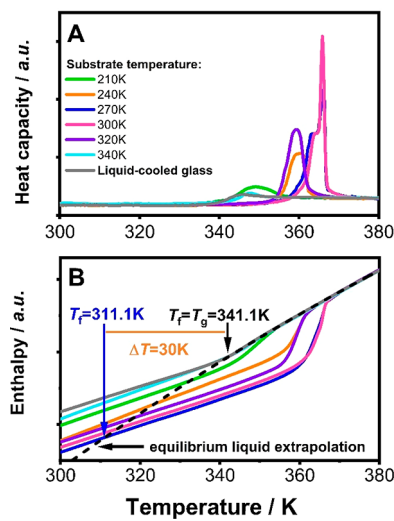


Figure 2. A) DSC heating curves for m-MTDATA/TPD mixtures codeposited at different temperatures. The gray curve denotes the result of the ordinary liquid-cooled glass; B) The enthalpy as a function of temperature for the studied m-MTDATA/TPD glasses. The heat capacity of the samples shown in panel A is integrated to obtain the enthalpy data, providing access to the fictive temperature for each sample. The dashed line is the extrapolation of the equilibrium liquid enthalpy to lower temperature by fitting the enthalpy data above  $T_g$  (from 345 to 380 K) to a quadratic function.

178 results from ellipsometry measurements are shown in Figure 178  
 179 S3. As seen from Figure 2A, the  $T_{\text{onset}}$  values for deposited 179  
 180 glasses varies substantially with the substrate temperature used 180  
 181 to prepare the glasses. This demonstrates that the kinetic 181  
 182 stabilities of codeposited m-MTDATA/TPD glasses are 182  
 183 controlled by the substrate temperatures, consistent with the 183  
 184 surface equilibration mechanism. 184

185 Figure 2A also indicates that the enthalpy for codeposited 185  
 186 m-MTDATA/TPD glasses with the same chemical composi- 186  
 187 tion is tunable. One may see that the glass transition 187  
 188 endothermic peak area is not constant when the glass mixtures 188  
 189 are deposited at different  $T_{\text{sub}}$ . The endothermic peak area 189  
 190 quantifies the enthalpy required to transform the glass into an 190  
 191 equilibrium liquid state. Figure 2B shows the enthalpy for 191  
 192 codeposited m-MTDATA/TPD glasses as determined by 192  
 193 integrating the heat capacity data in Figure 2A. Excluding 193  
 194 the glass deposited at  $T_{\text{sub}} = 340$  K, the enthalpy of 194  
 195 codeposited glasses is significantly lower than that of the 195  
 196 liquid-cooled glass. 196

197 The thermodynamic stability of codeposited m-MTDATA/ 197  
 198 TPD glasses can be quantitatively compared to single- 198  
 199 component PVD glasses using the fictive temperature  $T_f$ .<sup>11</sup> 199  
 200 As shown in Figure 2B, the  $T_f$  values for codeposited m- 200  
 201 MTDATA/TPD glasses were determined from the temper- 201  
 202 (extrapolated) enthalpy data for the equilibrium liquid (the 203  
 203 black curve). The m-MTDATA/TPD glass deposited at  $T_{\text{sub}} =$  204  
 204 270 K has the lowest  $T_f = 311.1$  K, which is 30 K lower than 205  
 205 that of the ordinary liquid-cooled glass with  $T_f = T_g = 341.1$  K. 206  
 206 This result is comparable to the most stable PVD glasses of 207  
 207 pure TNB<sup>11</sup> and IMC,<sup>39</sup> as well as amber glasses aged for tens of 208  
 208 millions of years<sup>40,41</sup> whose  $T_f$  values are around 30 K lower 209  
 209 than the glass transition temperature of the liquid-cooled glass. 210

211 Figure 3 demonstrates that the kinetic and thermodynamic 211 f3  
 212 stabilities of codeposited m-MTDATA/TPD glasses are 212  
 213 correlated. As shown in this figure, codeposited m- 213  
 214 MTDATA/TPD glasses with higher  $T_{\text{onset}}/T_g$  (i.e., higher 214  
 215 kinetic stability) have lower  $T_f/T_g$  (i.e., lower thermodynamic 215  
 216 energy state). The highest  $T_{\text{onset}}/T_g$  and lowest  $T_f/T_g$  values 216

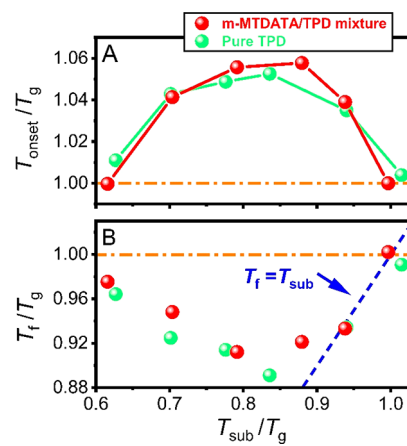
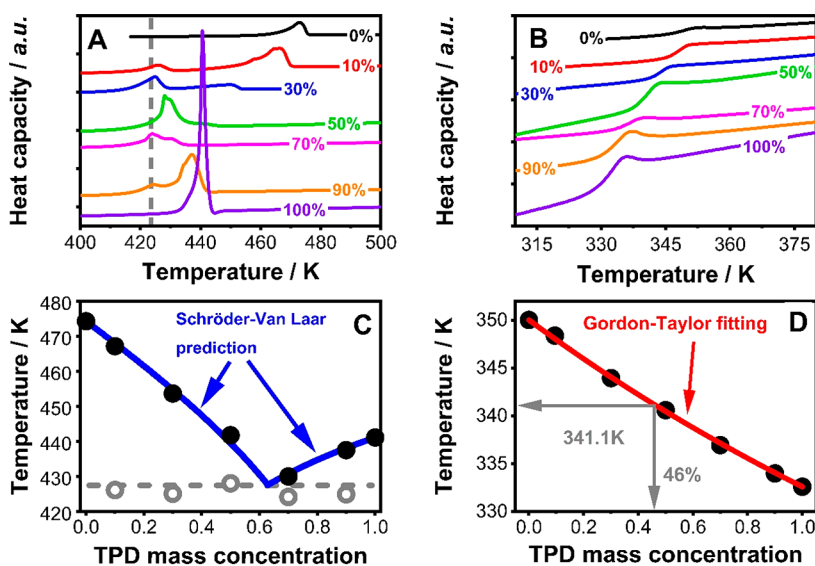


Figure 3. A) DSC results of  $T_{\text{onset}}/T_g$  for deposited m-MTDATA/ 217  
 218 TPD mixtures (red) and neat TPD (light green) glasses. The solid 218  
 219 lines are guides to the eye; B) DSC results of  $T_f/T_g$  for deposited m- 219  
 220 MTDATA/TPD mixtures (red) and neat TPD (light green) glasses. 220  
 221 The blue dashed line represents the  $T_{\text{sub}} = T_f$  line. The DSC heating 221  
 222 curves for as-deposited TPD glasses and the corresponding enthalpy 222  
 223 data are displayed in Figure S4. 223



**Figure 4.** A) Differential scanning calorimetry thermograms of the crystalline physical mixtures of m-MTDATA/TPD with different compositions. The percentages denote the corresponding mass concentration of the TPD. B) The glass transition region is for m-MTDATA/TPD mixtures with different compositions. C) Phase diagram of m-MTDATA/TPD mixtures using experimentally determined data (circles) and a fit to the Schröder–Van Laar equation (blue curves). D) The glass transition temperature of m-MTDATA/TPD mixtures as a function of mass concentration of TPD. The black circles are experimental data determined from panel B and the red curve is a fit to the Gordon–Taylor equation.

217 are obtained simultaneously when m-MTDATA/TPD glasses  
 218 are prepared at  $T_{\text{sub}} = 0.78\text{--}0.90T_g$ . These results indicate that  
 219 the kinetic stability of ultrastable m-MTDATA/TPD glasses is  
 220 coupled with the occurrence of low energy packing arrange-  
 221 ments. Although this behavior has been observed in single-  
 222 component organic vapor-deposited glasses,<sup>9,38,42</sup> it should be  
 223 noted that this is not a general feature for PVD glasses. For  
 224 example, the ternary metallic glass of  $\text{Zr}_{65}\text{Cu}_{27.5}\text{Al}_{7.5}$  deposited  
 225 at  $0.8T_g$  has an enhanced kinetic stability and elastic modulus  
 226 but an enthalpy higher than the corresponding liquid-cooled or  
 227 annealed glasses.<sup>17</sup>

228 Moreover, the determined trends of  $T_{\text{onset}}/T_g$  and  $T_f/T_g$  as a  
 229 function of  $T_{\text{sub}}/T_g$  for codeposited m-MTDATA/TPD  
 230 mixtures are in good agreement with those for most organic  
 231 single-component PVD glasses.<sup>9,38,42</sup> As an example for  
 232 comparison, we added the  $T_{\text{onset}}/T_g$  and  $T_f/T_g$  values for  
 233 vapor-deposited TPD glasses into Figure 3A and 3B. These  
 234 values are determined on the basis of the DSC measurements.  
 235 The corresponding heat capacity and enthalpy data are listed in  
 236 Figure S4. As seen from Figure 3, the data points of  $T_{\text{onset}}/T_g$   
 237 (or  $T_f/T_g$ ) as a function of  $T_{\text{sub}}/T_g$  for m-MTDATA/TPD  
 238 mixtures (red points) exhibit the same pattern as those for  
 239 pure TPD (light green points). Importantly, similar results are  
 240 obtained using spectroscopic ellipsometry (Figure S5).

241 The nonmonotonic dependence of  $T_{\text{onset}}/T_g$  and  $T_f/T_g$  on  
 242  $T_{\text{sub}}/T_g$  revealed in Figure 3 can be understood as a result of  
 243 the surface equilibration process during deposition. When the  
 244 layer is deposited below  $T_g$ , there is a thermodynamic driving  
 245 force to reach the equilibrium liquid state at that temperature.  
 246 High surface mobility enables molecules to find low energy and  
 247 high stability configurations before being buried (and  
 248 immobilized) by further deposition. Direct evidence for this  
 249 view is presented in Figure 3B; the fictive temperature for m-  
 250 MTDATA/TPD glasses deposited at  $0.94T_g$  is equal to the  
 251 corresponding substrate temperature (the blue dashed line  
 252 shows  $T_{\text{sub}} = T_f$ ). At lower values of  $T_{\text{sub}}/T_g$ , there will be a  
 253 larger thermodynamic driving force to form equilibrium state,  
 254 but simultaneously, the surface mobility will decrease. The

255 most stable glasses with the highest  $T_{\text{onset}}$  (or lowest  $T_f$ ) are  
 256 formed when high surface mobility is paired with a large  
 257 thermodynamic driving force. For organic semiconductor  
 258 compounds deposited at normal rates around  $0.1\text{--}1\text{ nm/s}$ ,  
 259 this match typically occurs when  $T_{\text{sub}}$  is around  $0.78\text{--}$   
 260  $0.90T_g$ .<sup>36,38</sup> At substrate temperatures lower than this, the  
 261 surface mobility is not so high, and only moderately stable  
 262 glasses are formed despite the presence of a larger driving  
 263 force. Our conclusion that the surface equilibration mechanism  
 264 explains the stability of codeposited glasses is consistent with  
 265 previous work that interpreted molecular  
 266 orientation in codeposited glasses using this mechanism.<sup>43,44</sup>

267 It is expected that the molecular interactions between the  
 268 two components will have a strong influence on the properties  
 269 of the binary PVD glasses. For example, strong repulsive  
 270 interaction may lead to component separation during  
 271 deposition, and strong attraction may inhibit surface diffusion.  
 272 For this reason, we investigated the miscibility of m-MTDATA  
 273 and TPD in bulk mixtures through calorimetric measurements.  
 274 Figure 4A illustrates the DSC results of the initial heating  
 275 process for binary crystalline physical mixtures of m-MTDATA  
 276 and TPD of different compositions. The percentages give the  
 277 mass concentration of TPD in each sample. Excluding pure  
 278 TPD (100% sample) and pure m-MTDATA (0% sample), two  
 279 melting processes are observed in all mixtures and the lower  
 280 melting point is independent of the compositions, indicating a  
 281 eutectic system. Based on these measurements, we constructed  
 282 the phase diagram of m-MTDATA/TPD mixtures. As seen in  
 283 Figure 4C, the experimental data are in good agreement with  
 284 the theoretical prediction from the Schröder–Van Laar  
 285 equation, indicating that this binary system is quite close to  
 286 an ideal mixture, which is miscible at any composition.  
 287

288 The glass transitions observed for these physical mixtures  
 289 provide important checks on miscibility and composition of  
 290 the PVD samples. As can be seen in Figure 4B, for each  
 291 mixture, a single glass transition is observed, demonstrating the  
 292 formation of a single glassy phase during cooling the molten  
 293 mixture. According to these DSC data, we determined the glass  
 294

293 transition temperature for m-MTADATA/TPD mixtures as a  
 294 function of the TPD concentration. As shown in Figure 4D,  
 295 the  $T_g$  values decrease monotonically with the increase of TPD  
 296 concentration, and the Gordon–Taylor equation<sup>45</sup> describes  
 297 the data well. Based on the Gordon–Taylor fitting curve, the  
 298 codeposited m-MTADATA/TPD glasses discussed above with  
 299  $T_g = 341.1$  K will contain 46% TPD, which is quite close to the  
 300 TPD concentration of 50% determined based on deposition  
 301 rate. We infer that the as-prepared PVD glasses are well-mixed,  
 302 based upon the single heat capacity maximum observed in the  
 303 DSC experiments (Figure 2A) and the observation that the use  
 304 of the mixture  $T_g$  in Figure 3 produces good correspondence  
 305 with single-component PVD glasses.

306 Sufficient surface mobility of both TPD and m-MTADATA  
 307 molecules at temperatures of interest is the key to forming  
 308 ultrastable codeposited m-MTADATA/TPD glass mixtures.  
 309 Figure 5 shows the experimental surface diffusion coefficients

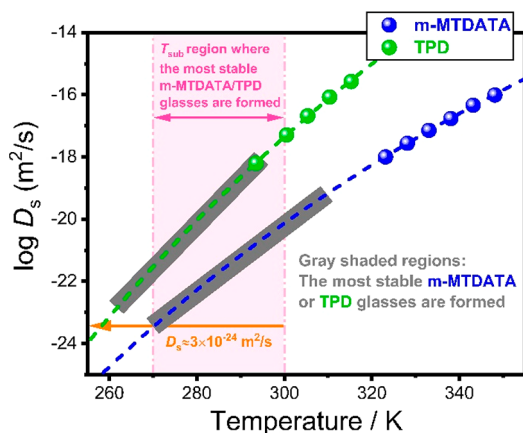


Figure 5. Surface diffusion coefficient of pure m-MTADATA (blue) and TPD (green) as a function of the absolute temperature. The  $D_s$  data for m-MTADATA and TPD were taken from ref 46 and ref 24, respectively. The dashed lines denote the Arrhenius extrapolation used to predict the  $D_s$  values at lower temperatures.

310 ( $D_s$ ) for pure TPD<sup>24</sup> and m-MTADATA<sup>46</sup> plotted as functions  
 311 of the absolute temperature. The Arrhenius equation was  
 312 applied to fit the data and extrapolated to lower temperatures.  
 313 The gray shaded portions of the extrapolated curves are the  
 314 regions where highly stable TPD or m-MTADATA glasses are  
 315 formed (using the criterion that  $T_{\text{onset}} / T_g \geq 1.05$  for TPD and  
 316  $T_{\text{onset}} / T_g \geq 1.04$  for m-MTADATA). Via this procedure, we  
 317 estimate that the minimum  $D_s$  required to form ultrastable neat  
 318 glasses of TPD and m-MTADATA is around  $3 \times 10^{-24} \text{ m}^2/\text{s}$ .  
 319 Interestingly, the  $D_s$  values for both TPD and m-MTADATA are  
 320 above  $3 \times 10^{-24} \text{ m}^2/\text{s}$  in the temperature region where the  
 321 most stable codeposited m-MTADATA/TPD glasses are formed  
 322 (the pink shaded region). If we assume that  $D_s$  for each  
 323 component in the mixture is not too different from the pure  
 324 component  $D_s$  values, our results can be rationalized by  
 325 concluding that both components in the codeposited mixture  
 326 must have surface mobility above some minimum value if a  
 327 stable glass is to be formed. When both components have high  
 328 mobility and  $T_{\text{sub}}$  is below the conventional glass transition  
 329 temperature of the corresponding mixtures, we expect that low  
 330 energy and high stability packing arrangements can be formed  
 331 during deposition. From this perspective, a major reason why  
 332 TPD and m-MTADATA can simultaneously have high mobility  
 333 at the same temperatures is their comparable glass transition

334 temperatures and ideal mixing. A mixture with strong attractive  
 335 interactions (nonideal mixing) might have lower surface  
 336 mobility that would interfere with stable glass formation, but  
 337 the nearly ideal nature of the m-MTADATA/TPD mixture rules  
 338 out this possibility. The arguments in this paragraph are based  
 339 upon the assumption that surface mobility of one component  
 340 is not perturbed by the presence of the second component. For  
 341 stable glass formation, this is the least optimiztic scenario. If,  
 342 for example, both components in a mixture were to have the  
 343 same (average) surface mobility, then it would not be  
 344 important that the two components had comparable  $T_g$  values.  
 345 Future work that provides guidance for understanding the  
 346 surface mobility of multicomponent systems would be very  
 347 useful.

348 So far, three works have investigated the stability of vapor-  
 349 deposited organic glass mixtures. In 2013, Whitaker et al.  
 350 reported highly stable glasses of *cis/trans*-decalin mixtures  
 351 across a range of compositions using *in situ* AC nano-  
 352 calorimetry;<sup>28</sup> the two isomers in this mixture have very similar  
 353 chemical structures and identical glass transition temperatures.  
 354 In 2018, Qiu et al. showed that PVD produced stable glasses of  
 355 5% 4,4'-diphenylazobenzene (DPA) with 95% celecoxib.<sup>29</sup>  
 356 The current work on m-MTADATA/TPD mixtures consid-  
 357 erably expands upon these two papers in using organic  
 358 semiconductor molecules that have different shapes and  $T_g$   
 359 values and shows that highly stable glasses are obtained even  
 360 for 50/50 mixtures. In 2022, Ki et al. reported an ellipsometric  
 361 study involving the stability of codeposited organic semi-  
 362 conductors.<sup>30</sup> They reported that codeposited Liq and BPhen  
 363 glasses across a wide mixing ratio did not show ultrastable  
 364 behavior when deposited at  $0.80T_g - 0.89T_g$ . We note that Ki et  
 365 al. also reported that pure Liq failed to form stable glasses via  
 366 PVD. We see this as a key difference as, for the mixtures  
 367 studied here, it has been confirmed experimentally that the two  
 368 pure components (i.e., TPD and m-MTADATA) can form  
 369 ultrastable glasses individually at proper deposition condi-  
 370 tions.<sup>36</sup> The inability of a pure component to form stable  
 371 glasses via PVD could be interpreted as a lack of surface  
 372 mobility, which might explain why mixtures involving that  
 373 component do not form stable glasses.

374 Given the large number of organic semiconductor mixtures  
 375 used as active layers and the importance of their stability in  
 376 electronic devices, it is useful to consider how general our  
 377 results may be. We conclude that the surface equilibration  
 378 mechanism controls the stability of codeposited m-MTADATA/  
 379 TPD glasses and suggest that the following three key features  
 380 are closely related to this conclusion: (i) both components can  
 381 form ultrastable glasses individually via PVD; (ii) the  
 382 components mix well at all compositions without strong  
 383 association; (iii) the glass transition temperature difference  
 384 between the components is not too large. Since many organic  
 385 semiconductors can form ultrastable glasses individually when  
 386 deposited under optimal conditions,<sup>36,38,47</sup> based on the  
 387 knowledge gained here, we expect that other organic  
 388 semiconductor mixtures can form ultrastable glasses when  
 389 the chosen compounds have properties similar to m-MTADATA  
 390 and TPD, including comparable glass transition temperatures,  
 391 high miscibility, and no strong association. In addition, we  
 392 anticipate that dilute mixtures of organic semiconductors,  
 393 which are widely used as light-emitter layers in OLED displays,  
 394 can form ultrastable glasses when deposited at around  $0.85T_g$   
 395 as sufficiently dilute solutions are always miscible. This  
 396 prediction is consistent with the work by Ràfols-Ribé et al.<sup>34</sup>

397 in which OLEDs containing a codeposited dilute mixture layer  
398 prepared at  $0.85T_g$  showed longer device lifetimes, if we  
399 assume that these longer lifetimes result from ultrastability.  
400 In summary, our work presents the first case of nondilute  
401 organic semiconductor glass mixtures with exceptional  
402 thermodynamic and kinetic stability. We demonstrate that  
403 the substrate temperature controls the stability of codeposited  
404 glasses of m-MTDATA and TPD in the same way as it controls  
405 the stability of single-component PVD organic glasses. For  
406 deposition near  $T_g$  the enthalpy is equal to that expected for  
407 the equilibrium liquid. Thus, the surface equilibration  
408 mechanism is extended to codeposited PVD glasses. We  
409 suggest that the main reasons why the PVD glasses of this  
410 binary system behave like a neat PVD glass are the ideal  
411 solution behavior and the comparable surface mobilities over  
412 the studied temperature range. In addition, both m-MTDATA  
413 and TPD are good glass formers and can individually form  
414 ultrastable glasses when deposited under proper conditions.  
415 Thus, they can be regarded as a model system to study the  
416 properties of binary PVD glasses of organic semiconductors.  
417 We expect that other organic semiconductor mixtures can form  
418 ultrastable glasses when the chosen compounds have proper-  
419 ties similar to m-MTDATA and TPD.

## 420 ■ ASSOCIATED CONTENT

### 421 ■ Supporting Information

422 The Supporting Information is available free of charge at  
423 <https://pubs.acs.org/doi/10.1021/acs.jpcllett.3c00728>.

424 Experimental materials and methods; GIWAXS patterns  
425 for codeposited m-MTDATA/TPD film (Figure S1);  
426 DSC results for codeposited m-MTDATA/TPD at  $T_{\text{sub}}$   
427 = 270 K (Figure S2); Normalized film thickness for  
428 codeposited m-MTDATA/TPD mixtures (Figure S3);  
429 DSC results for vapor-deposited TPD (Figure S4);  $T_{\text{onset}}$   
430 for vapor-deposited m-MTDATA/TPD mixtures and  
431 pure TPD (Figure S5) ([PDF](#))

## 432 ■ AUTHOR INFORMATION

### 433 Corresponding Author

434 M. D. Ediger – Department of Chemistry, University of  
435 Wisconsin-Madison, Madison, Wisconsin 53706, United  
436 States;  [orcid.org/0000-0003-4715-8473](https://orcid.org/0000-0003-4715-8473);  
437 Email: [ediger@chem.wisc.edu](mailto:ediger@chem.wisc.edu)

### 438 Authors

439 Shinian Cheng – Department of Chemistry, University of  
440 Wisconsin-Madison, Madison, Wisconsin 53706, United  
441 States;  [orcid.org/0000-0002-5615-8646](https://orcid.org/0000-0002-5615-8646)

442 Yejung Lee – Department of Chemistry, University of  
443 Wisconsin-Madison, Madison, Wisconsin 53706, United  
444 States

445 Junguang Yu – School of Pharmacy, University of Wisconsin-  
446 Madison, Madison, Wisconsin 53705, United States;  
447  [orcid.org/0000-0001-6458-8307](https://orcid.org/0000-0001-6458-8307)

448 Lian Yu – School of Pharmacy, University of Wisconsin-  
449 Madison, Madison, Wisconsin 53705, United States;  
450  [orcid.org/0000-0002-4253-5658](https://orcid.org/0000-0002-4253-5658)

451 Complete contact information is available at:

452 <https://pubs.acs.org/doi/10.1021/acs.jpcllett.3c00728>

### 453 Notes

454 The authors declare no competing financial interest.

## ■ ACKNOWLEDGMENTS

455 Work by Shinian Cheng, Yejung Lee, and M.D. Ediger was  
456 supported by the U.S. Department of Energy, Office of Basic  
457 Energy Sciences, Division of Materials Sciences and Engineer-  
458 ing, DE-SC0002161. Work by Junguang Yu and Lian Yu was  
459 supported by the NSF through the University of Wisconsin  
460 Materials Research Science and Engineering Center (Grant  
461 No. DMR-1720415). The use of the Stanford Synchrotron  
462 Radiation Lightsource, SLAC National Accelerator Laboratory,  
463 is supported by the U.S. Department of Energy, Office of  
464 Science, Office of Basic Energy Sciences, under Contract No.  
465 DE-AC02-76SF00515. 466

## ■ REFERENCES

(1) Ballato, J.; Dragic, P. Glass: the carrier of light—a brief history of optical fiber. *International Int. J. Appl. Glass Sci.* **2016**, *7*, 413–422. 468  
(2) Yu, L. Amorphous pharmaceutical solids: preparation, character- 469  
ization and stabilization. *Adv. Drug Delivery Rev.* **2001**, *48*, 27–42. 470  
(3) Shirota, Y.; Kageyama, H. Charge carrier transporting molecular 472  
materials and their applications in devices. *Chem. Rev.* **2007**, *107*, 473  
953–1010. 474  
(4) Schmidt, T. D.; Jäger, L.; Noguchi, Y.; Ishii, H.; Brüttig, W. 475  
Analyzing degradation effects of organic light-emitting diodes via 476  
transient optical and electrical measurements. *J. Appl. Phys.* **2015**, *117*, 477  
215502. 478  
(5) Bangsund, J. S.; Hershey, K. W.; Holmes, R. J. Isolating 479  
degradation mechanisms in mixed emissive layer organic light- 480  
emitting devices. *ACS Appl. Mater. Interfaces* **2018**, *10*, 5693–5699. 481  
(6) Hodge, I. M. Physical aging in polymer glasses. *Science* **1995**, 482  
267, 1945–1947. 483  
(7) Han, E. M.; Do, L. M.; Yamamoto, N.; Fujihira, M. 484  
Crystallization of organic thin films for electroluminescent devices. 485  
*Thin Solid Films* **1996**, *273*, 202–208. 486  
(8) Scholz, S.; Kondakov, D.; Lussem, B.; Leo, K. Degradation 487  
mechanisms and reactions in organic light-emitting devices. *Chem. 488  
Rev.* **2015**, *115*, 8449–8503. 489  
(9) Rodríguez-Tinoco, C.; Gonzalez-Silveira, M.; Ràfols-Ribé, J.; 490  
Garcia, G.; Rodríguez-Viejo, J. Highly stable glasses of celecoxib: 491  
Influence on thermo-kinetic properties, microstructure and response 492  
towards crystal growth. *J. Non Cryst. Solids* **2015**, *407*, 256–261. 493  
(10) Ramos, S. L. L.; Oguni, M.; Ishii, K.; Nakayama, H. Character 494  
of devitrification, viewed from enthalpic paths, of the vapor-deposited 495  
ethylbenzene glasses. *J. Phys. Chem. B* **2011**, *115*, 14327–14332. 496  
(11) Swallen, S. F.; Kearns, K. L.; Mapes, M. K.; Kim, Y. S.; 497  
McMahon, R. J.; Ediger, M. D.; Wu, T.; Yu, L.; Satija, S. Organic 498  
glasses with exceptional thermodynamic and kinetic stability. *Science* **499**  
*2007*, *315*, 353–356. 500  
(12) Raegen, A. N.; Yin, J.; Zhou, Q.; Forrest, J. A. Ultrastable 501  
monodisperse polymer glass formed by physical vapour deposition. 502  
*Nat. Mater.* **2020**, *19*, 1110–1113. 503  
(13) Jin, Y.; Zhang, A.; Wolf, S. E.; Govind, S.; Moore, A. R.; 504  
Zhernenkov, M.; Freychet, G.; Shamsabadi, A. A.; Fakhraai, Z. Glasses 505  
denser than the supercooled liquid. *Proc. Natl. Acad. Sci. U. S. A.* **2021**, 506  
*118*, e2100738118. 507  
(14) Qiu, Y.; Antony, L. W.; de Pablo, J. J.; Ediger, M. D. 508  
Photostability can be significantly modulated by molecular packing in 509  
glasses. *J. Am. Chem. Soc.* **2016**, *138*, 11282–11289. 510  
(15) Qiu, Y.; Dalal, S. S.; Ediger, M. D. Vapor-deposited organic 511  
glasses exhibit enhanced stability against photodegradation. *Soft 512  
Matter* **2018**, *14*, 2827–2834. 513  
(16) Luo, P.; Cao, C. R.; Zhu, F.; Lv, Y. M.; Liu, Y. H.; Wen, P.; Bai, 514  
H. Y.; Vaughan, G.; di Michiel, M.; Ruta, B.; Wang, W. H. Ultrastable 515  
metallic glasses formed on cold substrates. *Nat. Commun.* **2018**, *9*, 516  
1389. 517  
(17) Yu, H.-B.; Luo, Y.; Samwer, K. Ultrastable metallic glass. *Adv. 518  
Mater.* **2013**, *25*, 5904–5908. 519

520 (18) Dziuba, T.; Luo, Y.; Samwer, K. Local mechanical properties of 521 an ultrastable metallic glass. *J. Phys.: Condens. Matter* **2020**, *32*, 522 345101.

523 (19) Stevenson, J. D.; Wolynes, P. G. On the Surface of Glasses. *J. 524 Chem. Phys.* **2008**, *129*, 234514.

525 (20) Leonard, S.; Harrowell, P. Macroscopic Facilitation of Glassy 526 Relaxation Kinetics: Ultrastable Glass Films with Frontlike Thermal 527 Response. *J. Chem. Phys.* **2010**, *133*, 244502.

528 (21) Berthier, L.; Charbonneau, P.; Flenner, E.; Zamponi, F. Origin 529 of ultrastability in vapor-deposited glasses. *Phys. Rev. Lett.* **2017**, *119*, 530 188002.

531 (22) Bokas, G. B.; Zhao, L.; Morgan, D.; Szlufarska, I. Increased 532 stability of CuZrAl metallic glasses prepared by physical vapor 533 deposition. *J. Alloys. Compd.* **2017**, *728*, 1110–1115.

534 (23) Shi, Z.; Debenedetti, P. G.; Stillinger, F. H. Properties of Model 535 Atomic Free-Standing Thin Films. *J. Chem. Phys.* **2011**, *134*, 114524.

536 (24) Zhang, Y.; Potter, R.; Zhang, W.; Fakhraai, Z. Using tobacco 537 mosaic virus to probe enhanced surface diffusion of molecular glasses. 538 *Soft Matter* **2016**, *12*, 9115–9120.

539 (25) Zhu, L.; Brian, C. W.; Swallen, S. F.; Straus, P. T.; Ediger, M. 540 D.; Yu, L. Surface Self-Diffusion of an Organic Glass. *Phys. Rev. Lett.* 541 **2011**, *106*, 256103.

542 (26) Brian, C. W.; Yu, L. Surface self-diffusion of organic glasses. *J. 543 Phys. Chem. A* **2013**, *117*, 13303–13309.

544 (27) Zhang, Y.; Fakhraai, Z. Invariant fast diffusion on the surfaces 545 of ultrastable and aged molecular glasses. *Phys. Rev. Lett.* **2017**, *118*, 546 No. 066101.

547 (28) Whitaker, K. R.; Scifo, D. J.; Ediger, M. D.; Ahrenberg, M.; 548 Schick, C. Highly stable glasses of cis-decalin and cis/trans-decalin 549 mixtures. *J. Phys. Chem. B* **2013**, *117*, 12724–12733.

550 (29) Qiu, Y.; Antony, L. W.; Torkelson, J. M.; De Pablo, J. J.; Ediger, 551 M. D. Tenfold increase in the photostability of an azobenzene guest in 552 vapor-deposited glass mixtures. *J. Chem. Phys.* **2018**, *149*, 204503.

553 (30) Ki, M. S.; Sim, M.; Kwon, O.; Im, K.; Choi, B.; Cha, B. J.; Kim, 554 Y. D.; Jin, T. Y.; Paeng, K. Improved Thermal Stability and 555 Operational Lifetime of Blue Fluorescent Organic Light-Emitting 556 Diodes by Using a Mixed-Electron Transporting Layer. *ACS Mater. 557 Lett.* **2022**, *4*, 1676–1683.

558 (31) Jurow, M. J.; Mayr, C.; Schmidt, T. D.; Lampe, T.; Djurovich, 559 P. I.; Brüttig, W.; Thompson, M. E. Understanding and predicting 560 the orientation of heteroleptic phosphors in organic light-emitting 561 materials. *Nat. Mater.* **2016**, *15*, 85–91.

562 (32) Tenopala-Carmona, F.; Lee, O. S.; Crovini, E.; Neferu, A. M.; 563 Murawski, C.; Olivier, Y.; Zysman-Colman, E.; Gather, M. C. 564 Identification of the Key Parameters for Horizontal Transition Dipole 565 Orientation in Fluorescent and TADF Organic Light-Emitting 566 Diodes. *Adv. Mater.* **2021**, *33*, 2100677.

567 (33) Erickson, N. C.; Holmes, R. J. Highly efficient, single-layer 568 organic light-emitting devices based on a graded-composition 569 emissive layer. *Appl. Phys. Lett.* **2010**, *97*, 083308.

570 (34) Ràfols-Ribé, J.; Will, P. A.; Hänisch, C.; Gonzalez-Silveira, M.; 571 Lenk, S.; Rodríguez-Viejo, J.; Reineke, S. High-performance organic 572 light-emitting diodes comprising ultrastable glass layers. *Sci. Adv.* 573 **2018**, *4*, eaar8332.

574 (35) Bangsund, J. S.; Van Sambeek, J. R.; Concannon, N. M.; 575 Holmes, R. J. Sub-turn-on exciton quenching due to molecular 576 orientation and polarization in organic light-emitting devices. *Sci. Adv.* 577 **2020**, *6*, eabb2659.

578 (36) Walters, D. M.; Antony, L.; de Pablo, J. J.; Ediger, M. D. 579 Influence of molecular shape on the thermal stability and molecular 580 orientation of vapor-deposited organic semiconductors. *J. Phys. Chem. 581 Lett.* **2017**, *8*, 3380–3386.

582 (37) Rodríguez-Tinoco, C.; González-Silveira, M.; Barrio, M.; 583 Lloveras, P.; Tamarit, J. L.; Garden, J. L.; Rodríguez-Viejo, J. 584 Ultrastable glasses portray similar behaviour to ordinary glasses at 585 high pressure. *Sci. Rep.* **2016**, *6*, 34296.

586 (38) Dalal, S. S.; Walters, D. W.; Lyubimov, I.; de Pablo, J. J.; Ediger, 587 M. D. Tunable molecular orientation and elevated thermal stability of 588 vapor-deposited organic semiconductors. *Proc. Natl. Acad. Sci. U. S. A.* 589 **2015**, *112*, 4227–4232.

590 (39) Kearns, K. L.; Swallen, S. F.; Ediger, M. D.; Wu, T.; Sun, Y.; Yu, 591 L. Hiking down the energy landscape: Progress toward the Kauzmann 592 temperature via vapor deposition. *J. Phys. Chem. B* **2008**, *112*, 4934– 593 4942.

594 (40) Zhao, J.; Simon, S. L.; McKenna, G. B. Using 20-million-year- 595 old amber to test the super-Arrhenius behaviour of glass-forming 596 systems. *Nat. Commun.* **2013**, *4*, 1783.

597 (41) Pérez-Castañeda, T.; Jiménez-Riobóo, R. J.; Ramos, M. A. 598 Two-level systems and boson peak remain stable in 110-million-year- 599 old amber glass. *Phys. Rev. Lett.* **2014**, *112*, 165901.

600 (42) Ràfols-Ribé, J.; Gonzalez-Silveira, M.; Rodríguez-Tinoco, C.; 601 Rodríguez-Viejo, J. The role of thermodynamic stability in the 602 characteristics of the devitrification front of vapour-deposited glasses 603 of toluene. *Phys. Chem. Chem. Phys.* **2017**, *19*, 11089–11097.

604 (43) He, S.; Pakhomenko, E.; Holmes, R. J. Process Engineered 605 Spontaneous Orientation Polarization in Organic Light-Emitting 606 Devices. *ACS Appl. Mater. Interfaces* **2023**, *15*, 1652–1660.

607 (44) Jiang, J.; Walters, D. M.; Zhou, D.; Ediger, M. D. Substrate 608 temperature controls molecular orientation in two-component vapor- 609 deposited glasses. *Soft Matter* **2016**, *12*, 3265–3270.

610 (45) Gordon, M.; Taylor, J. S. Ideal copolymers and the second- 611 order transition of synthetic rubbers, I. non-crystalline copolymers. *J. 612 Appl. Chem.* **1952**, *2*, 493–500.

613 (46) Li, Y.; Bishop, C.; Cui, K.; Schmidt, J. R.; Ediger, M. D.; Yu, L. 614 Surface diffusion of a glassy discotic organic semiconductor and the 615 surface mobility gradient of molecular glasses. *J. Chem. Phys.* **2022**, 616 *156*, No. 094710.

617 (47) Dawson, K.; Zhu, L.; Kopff, L. A.; McMahon, R. J.; Yu, L.; 618 Ediger, M. D. Highly stable vapor-deposited glasses of four tris- 619 naphthylbenzene isomers. *J. Phys. Chem. Lett.* **2011**, *2*, 2683–2687.